Superconductivity at 9 K in Pb-Bi Alloy

N. K. Karn[1,2,*], Kapil Kumar[1,2], Naveen Kumar[1,2] Yogesh Kumar[1,2] and V.P.S. Awana[1,2,*]

[1]Academy of Scientific & Innovative Research (AcSIR), Ghaziabad, 201002, India
[2]CSIR- National Physical Laboratory, New Delhi, 110012, India

Abstract

In the present work, we report the synthesis of Pb-Bi alloy with enhanced T_c up to 9K, which is higher than that of Pb. The alloy is synthesized via solid-state reaction route in vacuum encapsulated quartz tube at 700^0C in an automated furnace. The synthesized sample is characterized by X-ray Diffraction for its phase purity. Rietveld refinement of XRD reveals that the end product is majority hexagonal Pb_7Bi_3, with minor rhombohedral Bi. The electronic transport measurement shows metallic behavior with the Debye temperature of 108K and a superconductivity transition temperature (T_c) at below 9K, which is maximum till date for any reported Pb-Bi alloy, Pb or Bi at ambient pressure . It is possible that partial substitution of Bi at the Pb site, modifies the free density of electronic states within BCS model to attain the optimum T_c, which is higher by around 2K from the reported T_c of Pb. The superconductor phase diagram derived from magneto-transport measurements reveals that the synthesized alloy is a conventional superconductor with upper critical field (H_c) of 3.9Tesla, which lies well within the Pauli paramagnetic limit.

Keywords: Superconductivity, Critical Transition temperature (T_c), Electrical Transport, Magneto-transport,

*Corresponding Author

Dr. V. P. S. Awana, Chief Scientist
CSIR-National Physical Laboratory, India
E-mail: aawana@nplindia.org
Ph. +91-11-45609357, Fax-+91-11-45609310

Introduction

Superconductivity has been one of the most intriguing phenomena since its discovery in 1911 and since then massive progress has been made from the phenomenological point of view and on its microscopic origin [1]. Among the various superconducting materials, superconductivity in alloys like HgAu, HgCd and PbSn [2] was discovered soon after the superconductivity found in Hg. The superconducting properties in alloys are tunable and can be engineered by varying alloy compositions [3, 4]. Recently, alloys of TaHf and TaZr have been shown to have applications in superconducting devices [5].

Among different alloy systems, the lead-bismuth (PbBi) alloys have attained significant interest due to their interesting electronic, topological [6, 7], and superconducting properties [8-10]. The combination of lead and bismuth in these alloys can offer promising avenues for exploring fundamental physics and practical applications like tuning superconductivity by atomically controlled thin film growth [11]. In this context, our research focuses on synthesizing Pb-Bi alloys via solid-state reaction method and characterizing their properties [12], particularly investigating their superconducting behaviour.

Recent studies have revealed fascinating aspects of Pb-Bi alloys. The transformation in crystal structure and superconducting behaviour have been investigated by varying the lead concentration in Pb-Bi alloy [13]. The alloy is found to be s-wave superconductor with its critical temperature depending upon the weight percentage of both elements in the alloy. Experimental efforts have explored the transport properties of Pb-Bi thin films grown by thermal evaporation, demonstrating the superconducting transition temperature and its dependence on applied magnetic field [14].

Pb-Bi alloys are significant because of their possible use in quantum technologies and superconducting devices [4, 15]. Considering the superconducting properties of Pb-Bi alloys, particularly their critical temperature, is crucial for advancing materials science and exploring unconventional superconductivity at lower temperatures.

In this article, we synthesized Pb-Bi alloys using a solid-state reaction method, followed by comprehensive characterization using X-ray diffraction (XRD) to determine their crystal structure. Our transport measurements revealed the superconducting nature of Pb-Bi with a critical

temperature (T_c) of 9 K. The upper critical field is calculated using GL theory formulation which is found to be higher compared to previous reports. This finding underscores the potential of Pb-Bi alloys for low-temperature superconducting applications and motivates further investigation into their underlying physical mechanisms.

Experimental

The alloy of Pb-Bi is prepared in a single step by following the solid-state reaction route. High-purity (>4 N) powders of Pb and Bi were taken into the stoichiometric ratio 1:1. These powders were mixed and ground thoroughly by using an agate mortar pestle in an argon-filled glove box. This homogenous mixture was then palletized and vacuum encapsulated at a pressure of 5×10^{-5} mbar. This vacuum-encapsulated sample was then placed into an automated PID-controlled Muffle furnace subjected to the heat treatment shown in Fig.1. The encapsulated pallet is heated to 700°C at a rate of 60°C/h. This sample is kept at this elevated temperature for 48h and then cooled normally to room temperature. As obtained crystalline Pb-Bi alloy is shown in the inset of Fig.1. Rigaku mini flex tabletop X-ray diffractometer (XRD) equipped with Cu-K$_\alpha$ radiation of wavelength 1.54 Å is used to record the XRD pattern of the synthesized alloy Pb-Bi. Electrical transport measurements have been carried out using a Quantum Design (QD) made Physical Property Measurement System (PPMS) with the sample mounted on a PPMS DC puck. A standard four-probe method has been used for the magneto transport measurements, in which four linear contacts with silver epoxy have been made on the surface of the sample.

Results and Discussion

After heat treatment, the obtained crystals are silvery shiny and around 1cm long as shown in the inset of Fig. 1. Fig. 2(a) exhibits the Rietveld refined powder XRD (PXRD) pattern of synthesized Pb-Bi alloy which fits in two phases Pb_7Bi_3 and Bi. The Pb_7Bi_3 crystallizes in a hexagonal phase with P63/mmc space group, whereas Bi has a rhombohedral structure with space group R-3m. The goodness of fit parameter, i.e., $\chi2$ is found to be 6.89 which is reasonable. The obtained lattice parameters are a=b= 3.502(1)Å and c= 5.791(8)Å, and α=β=90, γ=120° for Pb_7Bi_3 and the same for Bi is obtained as a=b= 4.539(4)Å and c= 11.859(5)Å and α=β=90, γ=120°. The obtained lattice parameters are found close to the previous reports [13, 16]. The results of powder XRD refinement are summarized in Table 1. All observed peaks in the PXRD pattern are spaned by the Bragg position generated by the two phases and corresponding to the observed peaks, and

planes are marked for both Pb_7Bi_3 and Bi. The inset in the Fig. 2(a) shows the VESTA-drawn unit cell of both phases present in the alloy with the refined lattice parameters.

Next, the electronic and magneto-transport properties of the as-synthesized Pb-Bi alloy have been studied by performing transport measurements on PPMS. Fig. 3 shows the resistivity vs temperature (ρ-T) plot at zero magnetic field. A superconducting transition is observed (see inset of Fig. 3) as the resistivity starts decreasing sharply at $T_c^{onset} = 9\pm0.2$ K, which is close to the previously reported values [13, 17]. The temperature at which $\rho = 0$ (T_c^{offset}) is seen, is at 8.7 ± 0.2 K, with a transition width of ~0.3 K. Above T_c, the resistivity increases with temperature, showing high metallicity of the synthesized crystal. Above T_c (i.e., 9K–300 K) the ρ–T data are fitted using the Bloch–Grüneisen formula given below

$$\rho(T) = \rho(0) + \rho_{el-ph}(T) \tag{1}$$

Here, $\rho(0)$ denotes residual resistivity arising due to impurity scattering and $\rho_{el-ph}(T)$ denotes the temperature-dependent term, which depends on electron-phonon scattering. Furthermore, $\rho_{el-ph}(T)$ is given by the following formula:

$$\rho_{el-ph} = \alpha_{el-ph} \left(\frac{T}{\theta_D}\right)^n \int_0^{\frac{\theta_D}{T}} \frac{x^n}{(1-e^{-x})*(e^x-1)} dx \tag{2}$$

Here, α_{el-ph} is the electron-phonon coupling parameter, θ_D represents the Debye temperature, and n is a constant. The ρ–T data are well fitted for n = 5, signifying dominant electron-phonon scattering above T_c. The deduced values are $\theta_D = 107.72$ K and $\rho(0) = 0.159$ $\mu\Omega$-cm. The residual resistivity ratio (RRR) given by $\rho(300K)/\rho(Tc)$ is ~1.88. The resistivity of the synthesized alloy is of the order of $10^{-7}\Omega$-cm which is lower than Copper. This endorses the quality and the high metallicity of the synthesized Pb-Bi alloy.

To study the upper critical field and other superconducting parameters of the synthesized alloy, magnetotransport measurements have been performed. Fig. 4(a) depicts ρ-T plots in the temperature range 2K-15K at different fields. We observe that, for low fields the superconductor transition is sharp but at higher fields, the transition width increases. Fig. 4(b) illustrates the resistivity vs field ρ-H plot with applied field ±6 Tesla for different temperatures 2K to 10K at the interval of 0.5K. Similar to ρ-T plots, at lower temperatures, the gap in H_c^{onset} and H_c^{offset} increases. Using the data from Fig. 4(a) and (b), the superconducting phase diagram is produced

in the phase space of (T_c, H_c) as shown in Fig. 5. From the phase diagram, it is evident that the $\Delta H_c = H_c^{onset} - H_c^{offset}$ increases for lower temperatures. To find out the upper critical field of the as-synthesized Pb-Bi alloy, the phase diagram is extrapolated to 0K using the Gingberg-Landau model:

$$H_{c2}(T) = H_{c2}(0) \left[\frac{1-t^2}{1+t^2}\right] \tag{3}$$

Where $t=T/T_c$ is reduced temperature. The fitted data is shown in Fig. 5 by solid black lines. Using the extrapolation of the above-applied model, the upper critical fields are found to be $H_c^{onset}(0) = 3.91$ T and $H_c^{offset}(0) = 3.01$ T. To further calculate the superconducting parameters, Ginzburg-Landau (GL) formula for coherence length is used, where the upper critical field given by $H_{c2}(0) = \frac{\phi_0}{2\pi\xi_{GL}(0)^2}$, $\phi_0 = h/2e$ is the flux quantum and $\xi_{GL}(0)$ is the G-L coherence length at T= 0K. As a result, the G-L coherence length $\xi_{GL}(0)$ is found to be 9.17 nm and 10.45 nm, for H_c^{onset} and H_c^{offset}, respectively. The upper critical field is governed by the Pauli paramagnetic effect (H_p in tesla) which is limited by the Chandrasekhar-Clogston (or Pauli) paramagnetic limit, $H_p \equiv 1.86T_c$ at T=0 K [18]. For the synthesised Pb-Bi alloy, this limit is 16.74Tesla which is higher than the calculated upper critical field H_c. This indicates conventional BCS type superconductivity present in the sample. However, the upper critical field here reported is higher in comparison to the previous report. Previously, Pb-Bi alloy is reported to have a maximum $T_c \sim 8.7$K [13]. The Bi in single crystal form shows superconductivity at extremely low temperatures ($\sim$mK) [19], whereas the Bi nanoparticle exhibits T_c up to 8.75K [20]. The GL coherence length for our sample is smaller in comparison to superconducting Bi nanoparticles but comparable to that of Pb-Bi alloy reported by Gandhi et al [13]. Thus, in the synthesized Alloy of Pb-Bi alloy, the observed superconductivity is due to Pb_7Bi_3. In comparison to the previous reports, we have achieved higher T_c as well as upper critical field for the Pb-Bi alloy.

Conclusion

To summarise, here we report the successful growth of crystalline Pb-Bi alloy following a solid-state reaction route which contains two phases Pb_7Bi_3 (majority) and Bi (minority). The electronic transport ρ-T plot shows that the synthesized Pb-Bi alloy has T_c at 9K. The magnetotransport measurement was performed and the superconductor phase diagram

extrapolation resulted in the upper critical field to 3.9Tesla at 0K. Further, by comparing the superconducting parameters obtained by the phase diagram, we conclude that the superconductivity shown by the synthesized alloy is due to the majority Pb_7Bi_3 phase.

Acknowledgment

Table 1

Parameters obtained from Rietveld refinement

Pb_7Bi_3	Bi	Refinement Parameters
Cell Parameters	Cell Parameters	
Cell type: Hexagonal Space Group: P63/mmc Lattice parameters: a=b=3.502((7)Å & c=5.791(8) Å $\alpha=\beta=90°$ & $\gamma=120°$ Atomic co-ordinates: Pb (0.3333,0.6666,0.25) Bi (0.6666,0.3333,0.75)	Cell type: Rhombohedral Space Group: R-3m (166) Lattice parameters: a=b=4.539(4)Å & c=11.859(5) Å $\alpha=\beta=90°$ & $\gamma=120°$ Atomic co-ordinates: Bi(0,0,0.2327)	$\chi^2=6.89$ $R_p=19.7$ $R_{wp}=26.6$ $R_{exp}=10.15$

Figure Captions

Figure 1: Heat treatment of the Pb-Bi alloy and inset shows the as-grown single crystal.

Figure 2: Rietveld refinement of PXRD pattern of synthesized Pb-Bi alloy. The inset shows the unit cell of both Pb_7Bi_3 and Bi generated by VESTA.

Figure 3: Temperature-dependent resistance of Pb-Bi alloy at zero field and the inset shows the enlarged image near the transition temperature.

Figure 4: (a) Show the temperature-dependent resistivity of Pb-Bi alloy for various applied fields. **(b)** The magnetic field dependence of the resistivity $\rho(H)$ in Pb-Bi alloy in temperature range 2-10K.

Figure 5: Variation of the critical field with reduced temperature for Pb-Bi alloy.

References:

1. Sigrist, M. and Ueda, K., Reviews of Modern physics, **63**(2), 239 (1991).

2. Webb, G.W., Marsiglio, F. and Hirsch, J.E., Physica C: Superconductivity and its applications, **514**, 17 (2015).

3. Sun, L. and Cava, R.J., Physical Review Materials, **3**(9), 090301 (2019).

4. Ozer, M.M., Jia, Y., Zhang, Z., Thompson, J.R. and Weitering, H.H., Science, **316**(5831), 1594 (2007).

5. Klimczuk, T., Królak, S. and Cava, R.J., Physical Review Materials, **7**(6), 064802 (2007).

6. Mihalyuk, A.N., Bondarenko, L.V., Tupchaya, A.Y., Utas, T.V., Vekovshinin, Y.E., Gruznev, D.V., Eremeev, S.V., Zotov, A.V. and Saranin, A.A., Physical Review B, **104**(12), 125413 (2021).

7. Bentaibi, B., Drissi, L.B., Saidi, E.H., Fassi-Fehri, O. and Bousmina, M., Materials Science in Semiconductor Processing, **174**, 108180 (2024).

8. Chang, M.S., Salleh, M.M. and Halin, D.S.C., In IOP Conference Series: Materials Science and Engineering, **957(**1), 012059 (2020).

9. Gordon, D.E. and Deaton, B.C., Superconductivity in metastable bismuth eutectic alloys. Physics Letters A, **27**(2), 116 (1968).

10. Rasmussen, S.E. and Lundtoft, B., Powder Diffraction, **2**(1)28 (1987).

11. Xie, K., Li, P., Liu, L., Zhang, R., Xia, Y., Shi, H., Cai, D., Gu, Y., She, L., Song, Y. and Zhang, W., Physical Review B, **107**(10), 104511 (2023).

12. Okayasu, S., Ono, M., Nishio, T., Iguchi, Y. and Mashimo, T., April. Separation in ε-Phase of BiPb Alloy under Mega-Gravity. In Defect and Diffusion Forum, **323**, 545(2012).

13. Gandhi, A.C., Chan, T.S. and Wu, S.Y., Superconductor Science and Technology, **30**(10), 105010 (2017).

14. Kuru, M., Ongun, E. and Ozmetin, A.E., Materials Research Express, **4**(6), 066001 (2017).

15. Jia, Y., Wang, S.Y., Chen, W.G., Sun, Q., Weitering, H.H. and Zhang, Z., Physical Review B, **81**(24), 245425 (2010).

16. Kumar, Y., Sharma, P., Karn, N.K. and Awana, V.P.S., Journal of Superconductivity and Novel Magnetism, **36**(2), 389 (2023).

17. Gandhi, A.C. and Wu, S.Y., Journal of Magnetism and Magnetic Materials, **407**, 155 (2016).

18. Lu, J.M., Zheliuk, O., Leermakers, I., Yuan, N.F., Zeitler, U., Law, K.T. and Ye, J., Science, **350**(6266), 1353 (2015).

19. Prakash, O., Kumar, A., Thamizhavel, A. and Ramakrishnan, S., Science, **355**(6320), 52(2017).

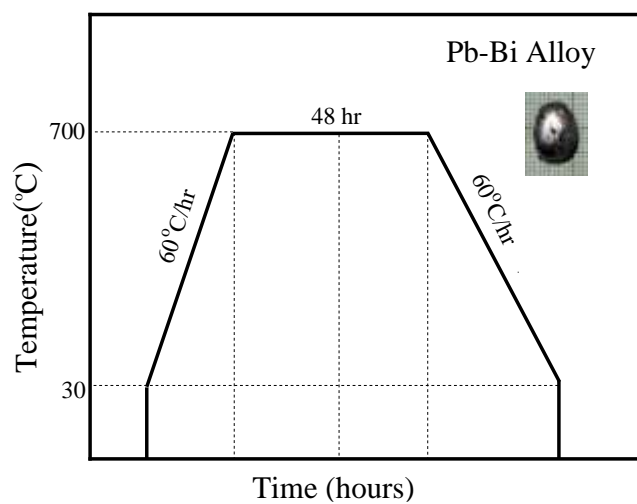20. Gandhi, A.C., Gaikwad, S.S., Peng, J.C., Wang, C.W., Chan, T.S. and Wu, S.Y., APL Materials, **7**(3)(2019).
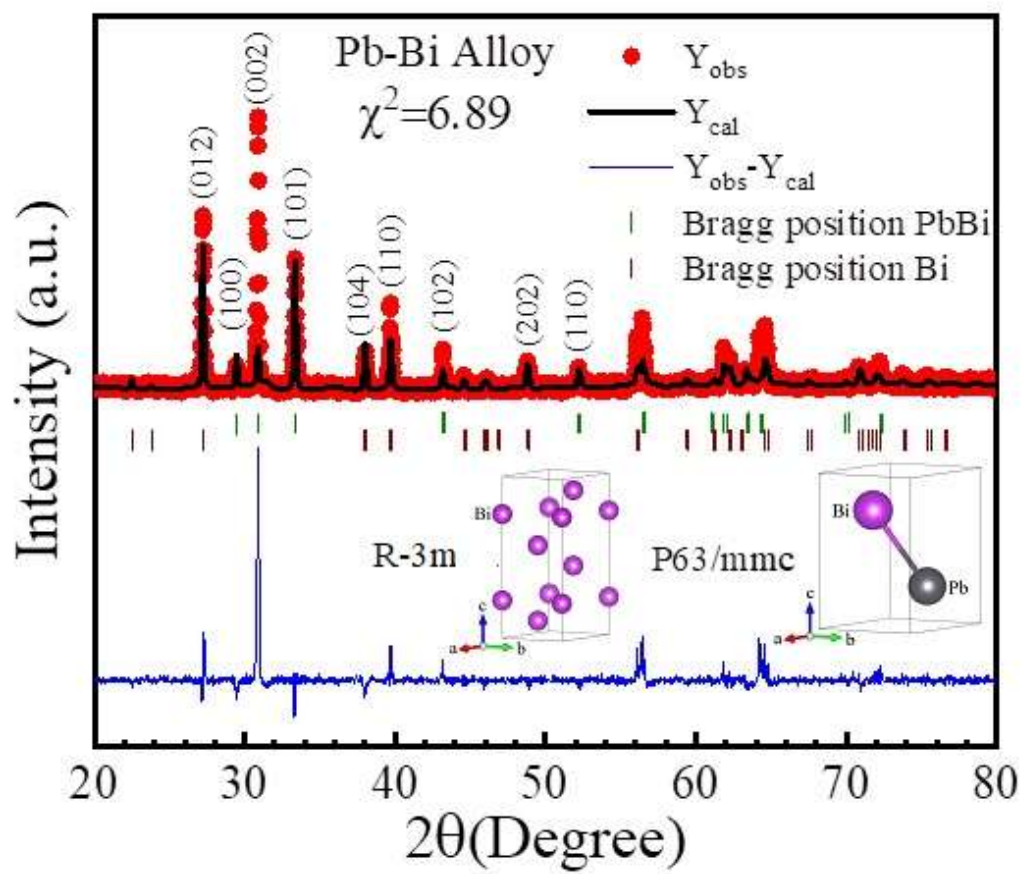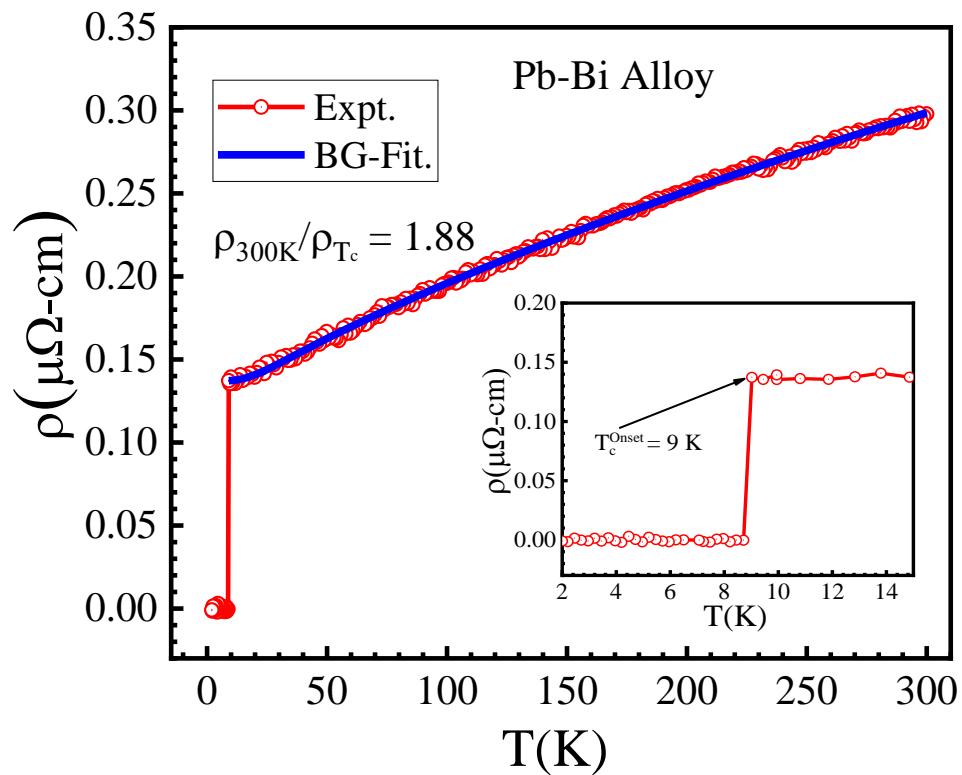
Figure 1:

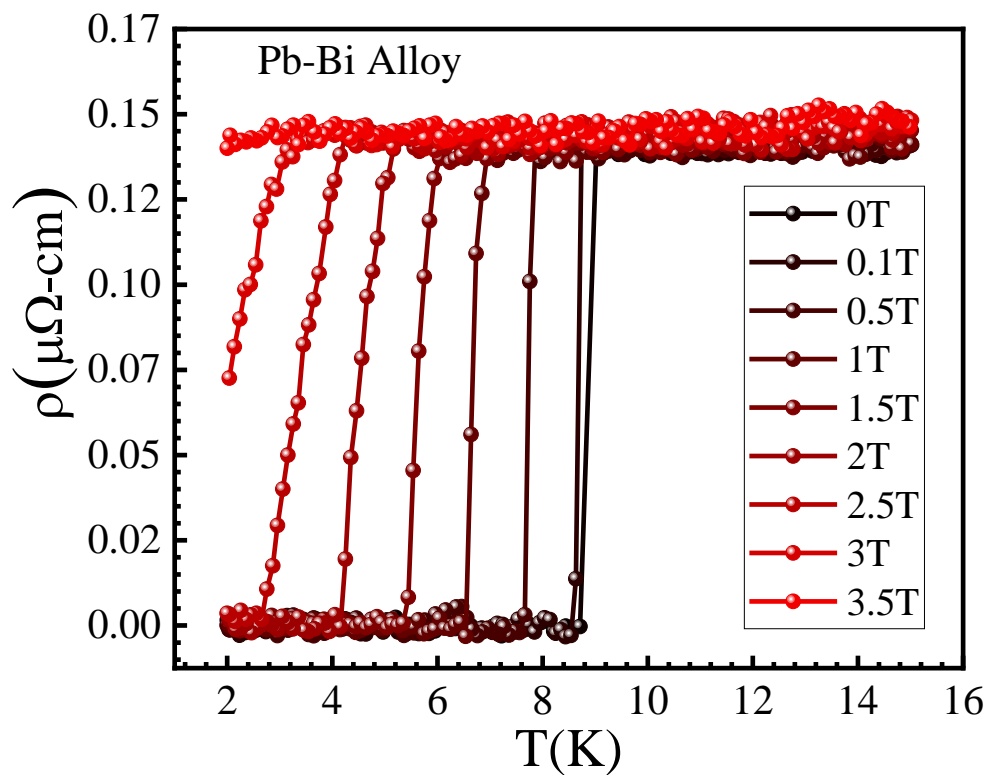Figure 2(a):

Figure 3:

Figure 4(a)

Figure 4(b)

Figure 5